Canadian Mineralogist
Vol. 25, pp. 515-525 (1987)

ULTRABASIC XENOLITHS FROM THE HAM KIMBERLITE, SOMERSET ISLAND, NORTHWEST TERRITORIES

BRUCE C. JAGO AND ROGER H. MITCHELL
Department of Geology, Lakehead University, Thunder Bay, Ontario P7B 5E1

ABSTRACT

The mantle-derived xenolith population found in the Ham kimberlite (Somerset Island, Northwest Territories) consists predominantly of coarse granular-, porphyroclastic- and mosaic-textured garnet lherzolite and subordinate, weakly deformed spinel lherzolite. Compositional data are presented for the constituent minerals of the lherzolites and used to calculate temperatures and pressures of equilibration. The variously textured garnet lherzolites have equilibrated over similar relatively limited ranges of temperature and pressure (coarse granular texture: 1022–1094°C, 35.5–38.4 kbar; porphyroclastic texture: 1038–1151°C, 35.7–40.2 kbar; mosaic texture: 927–1140°C, 32.5–39.5 kbar) that do not coincide with those of the theoretical steady-state shield geotherm and which lie outside of the diamond stability field. The wide range of equilibration temperatures determined for spinel lherzolites (262–1142°C) suggest that they represent disequilibrium assemblages. Garnet lherzolites are believed to be derived from a thermal aureole surrounding a mantle diapir. Deformation associated with crack formation and propagation above this diapir is considered to give rise to zones of mosaic- and porphyroclastic-textured lherzolite within an otherwise coarse granular-textured mantle. Sampling of this heterogeneous mantle by an ascending kimberlitic magma accounts for the observed suite of xenoliths.

Keywords: kimberlite, garnet lherzolite, spinel lherzolite, geothermobarometry, Somerset Island, Northwest Territories.

SOMMAIRE

La population de nodules dérivés du manteau dans la kimberlite de Ham, sur l'île de Somerset, aux Territoires du Nord-Ouest, contient surtout des lherzolites à grenat granulaires à granulométrie grossière, porphyroclastiques ou à texture mosaïque, ainsi que des lherzolites à spinelle faiblement déformés. L'information sur la composition chimique des minéraux des lherzolites sert à calculer leurs températures et pressions d'équilibrage. Les lherzolites à grenat ont atteint l'équilibre sur un intervalle relativement restreint de température et de pression (texture granulaire à gros grains: 1022–1094°C, 35.5–38.4 kbar; texture porphyroclastique: 1038–1151°C, 35.7–40.2 kbar; texture mosaïque: 927–1140°C, 32.5–39.5 kbar), valeurs qui ne coïncident pas avec celles prédites pour le géotherme stable de la région et qui sont en dehors du champ de stabilité du diamant. La grande variabilité dans les températures de ré-équilibrage des lherzolites à spinelle (262–1142°C) font penser qu'il s'agit d'assemblages en déséquilibre. Les lherzolites à grenat seraient dérivées d'une auréole de contact entourant un diapir dans le manteau. La déformation associée à la formation et à la propagation de fissures au-dessus de ce diapir aurait causé des zones de lherzolites à textures mosaïque et porphyroclastique dans un domaine autrement à granulométrie grossière. Un échantillonage de ce manteau hétérogène par le magma kimberlitique ascendant rend compte de la suite de nodules observés.

(Traduit par la Rédaction)

Mots-clés: kimberlite, lherzolite à grenat, lherzolite à spinelle, géothermobarométrie, île de Somerset, Territoires du Nord-Ouest.

INTRODUCTION

The Ham kimberlite is the northernmost manifestation of the Somerset Island kimberlite province (Mitchell 1976). It consists of a main bell-shaped intrusive body (Ham diatreme) and a single dyke (Ham dyke) located 1.5 km to the east. A detailed description of the mineralogy and petrology of the Ham kimberlite is given by Jago (1982) and Jago & Mitchell (1985).

Ovoid xenoliths of garnet and spinel lherzolite, up to 10 cm in diameter, were found within the regolith overlying the Ham diatreme and in an area of outwash occurring downslope from the intrusive body to the west. Although no lherzolite xenoliths were found in the Ham dyke, macrocrysts of chrome-diopside and Cr-rich, Ti-poor pyrope garnet were found in heavy-mineral concentrates from the kimberlite (Jago 1982), indicating that such xenoliths were fragmented during kimberlite emplacement.

Xenoliths of mantle-derived garnet and spinel lherzolite have been found at five other localities in the Somerset Island kimberlite province. Rare garnet lherzolites are present in the Ameyersuk, Tunraq and Inugpasugsuk kimberlites, but are more plentiful, with garnet lherzolite predominating over spinel lherzolite, in the Elwin Bay and Nanorluk kimberlites (Mitchell 1978, 1987). At the Ham kimberlite, garnet lherzolites are the most abundant type of xenolith found.

PETROGRAPHY OF THE XENOLITHS

The Ham lherzolites may be classified texturally using the scheme of Harte (1977). A complete gradation in textural type exists between coarse granular-, porphyroclastic-, and mosaic-textured xenoliths. A single granuloblastic xenolith was found. Porphyroclastic xenoliths appear to be the most common, and several mosaic types exhibit protolaminated textures. Minerals in individual xenoliths are generally well preserved; serpentinization, where present, is confined to a narrow (<1 cm thick) alteration selvage on most xenoliths and commonly is developed in cataclastic zones in mosaic-textured xenoliths.

Garnet lherzolite

Coarse granular garnet lherzolite is composed essentially of anhedral, tabular colorless olivine and orthopyroxene, with lesser (<5 vol.%) tabular to equant, pale to dark green clinopyroxene and round garnet. Grain boundaries between olivine and pyroxene generally are straight to slightly curving; the garnet has a thick kelyphitic rim. Deformation textures (subgrains, strain twins, undulose extinction, kink banding) in olivine are generally confined to strain shadows associated with large grains of garnet.

In moderately deformed xenoliths, the grain size of porphyroclastic olivine decreases, and olivine and orthopyroxene no longer form a tight interlocking framework. Olivine occurs in three habits, as subtabular to subovoid porphyroclasts, as anhedral subgrains and as subhedral neoblasts. Deformation textures are strongly developed in olivine porphyroclasts. These textures are confined to discontinuous, subparallel cataclastic zones and strain shadows around garnet and multigrain aggregates of pyroxene. Olivine neoblasts usually are elongate parallel to cataclastic zones but are not always confined to zones of strong deformation. Individual grains are strain-free. Straight grain-boundaries commonly meet to form triple junctions with other neoblasts. Orthopyroxene and clinopyroxene occur as coarse, relatively undeformed tabular to subequant grains. Garnet occurs as round porphyroclasts with weakly to strongly developed kelyphite.

In several xenoliths, the kelyphite mantle is overgrown by a thin discontinuous rim of light to dark brown phlogopite, rare spinel and very rare clinopyroxene. The phlogopite is optically continuous over significant distances around each garnet grain but also occurs rarely as stubby interlocking crystals. Spinel in the phlogopite rim occurs as discrete euhedral crystals or as acicular intergrowths parallel to the {001} cleavage of the mica. The dark green clinopyroxene is anhedral in habit and confined to the outer reaction-interface. In the rare instances that these mantles were observed, they are developed preferentially against granular to porphyroclastic olivine and, in one instance, against olivine subgrains and neoblasts in a cataclastic zone.

Similar mantles of phlogopite have been described by Carswell (1975), Delaney *et al.* (1980), Schandl & Clarke (1982) and Mitchell (1984). The Ham lherzolites differ from these in that veins and "pools" of similar mineralogy are lacking elsewhere in the xenolith.

Mosaic porphyroclastic- to mosaic-textured xenoliths occur in two parageneses, as multigrain aggregates of porphyroclastic olivine with lesser orthopyroxene and clinopyroxene, and as single grains of porphyroclastic olivine and garnet supported by a framework of olivine subgrains and neoblasts. Deformation textures characteristic of highly deformed olivine in porphyroclastic xenoliths are less common in mosaic-textured xenoliths, presumably owing to a relaxation of strain accompanying subgrain formation (Kretz 1966). Orthopyroxene and clinopyroxene occur as generally coarse-grained subequant to subtabular and subequant to lobate grains, respectively, and demonstrate only weak to moderate undulose extinction. Garnet is much smaller in mosaic-textured xenoliths (1 mm *versus* 4 mm) relative to granular and porphyroclastic types, presumably owing to the dismemberment of the parental porphyroclast. Garnet subgrains typically are "quarter moon"-shaped and strongly kelyphitized, whereas rare relatively round porphyroclasts are weakly kelyphitized.

The single granuloblastic xenolith (Ham 006) consists of roughly equant, polygonal subgrains and neoblasts of olivine, rare subtabular porphyroclastic olivine and lesser subequant to tabular, weakly porphyroclastic orthopyroxene and clinopyroxene. The two pyroxenes occur in protolaminations with remnant porphyroclastic olivine and are supported by a framework of olivine subgrains and neoblasts. Within the latter occur strongly kelyphitized "quarter-moon"-shaped and round garnet porphyroclasts.

Intrasilicate inclusions in the garnet lherzolites

Olivine, clinopyroxene, rare orthopyroxene and garnet occur as single, small, rounded inclusions in other silicate grains. Olivine followed by clinopyroxene is the most common inclusion, both phases preferentially occurring in garnet compared to orthopyroxene (ratio 9:1). A single rounded grain each of orthopyroxene and garnet was found in porphyroclastic olivine, both in strongly deformed garnet lherzolites. Included phases almost invariably are round and always in equilibrium contact with their host, and do not appear to be connected to the margin of the host by fractures. This feature and the rounded nature of the inclusions suggest that they were primary phases formed in the xenolith prior to their host and subsequently overgrown, possibly during a later deformation or metasomatic event.

Spinel lherzolite

The two xenoliths of spinel lherzolite (Ham 051, 071) are weakly porphyroclastic and consist of weakly deformed olivine and orthopyroxene and subordinate clinopyroxene and an opaque phase. Most silicate grains demonstrate weak to moderate undulose extinction and kink banding. Strongly deformed grains of orthopyroxene have exsolved fine lamellae of clinopyroxene. Grains of pale and medium dark green clinopyroxene, where strongly deformed, have exsolved fine lamellae of orthopyroxene. In contrast to pale green types, dark green clinopyroxene exhibits a disequilibrium contact with other silicate phases. Contact zones are typically irregular and turbid; in Ham 051, tiny euhedral grains of aluminous magnesian chromite have developed. These grains of spinel are compositionally similar to the intergranular spinel. The latter occur as round to ovoid intergranular opaque grains. The spinel grains in Ham 071 occur as intergranular, translucent, orange-brown to reddish brown, cuspate grains. Typically contacts are round and embayed, large grains partly engulfing small- to medium-sized silicate grains.

MINERAL CHEMISTRY

All minerals were analyzed at Dalhousie University using a Cambridge MK V microprobe (EDS) and natural standards. Raw X-ray intensities were corrected using EDATA 2. Following Boyd & Finger (1975), average mineral compositions (Tables 1-6) are based upon three to six mineral analyses per sample. These averages have been used to estimate the temperatures and pressures of equilibration given in Table 7.

Olivine

The average composition of olivine in the garnet and spinel lherzolites is given in Table 1. Each xenolith has a relatively distinct compositional population of olivine, and there is no intraxenolith compositional variation among texturally similar grains of olivine. The olivine is extremely magnesium- and nickel-rich ($Fo_{90.0}$–$Fo_{92.5}$, 0.20–0.70 wt.% NiO). The nickel content demonstrates a positive correlation with increasing forsterite content. The coarse granular olivine in granular lherzolites is the most magnesium- and nickel-rich ($Fo_{91.5}$–$Fo_{92.5}$, av. 0.37 wt.% NiO), followed by porphyroclastic olivine in porphyroclastic ($Fo_{90.8}$–$Fo_{91.2}$, av. 0.29 wt.% NiO) and mosaic-textured xenoliths ($Fo_{91.1}$–$Fo_{91.9}$, av. 0.35 wt.% NiO). Olivine neoblasts are weakly magnesium- and nickel-rich compared to parental olivine in each textural type. The olivine that occurs as inclusions is compositionally similar to the average olivine in the host xenolith.

TABLE 1a. AVERAGE COMPOSITION OF OLIVINE IN HAM GARNET LHERZOLITE

#	SiO_2	TiO_2	Cr_2O_3	FeO*	MgO	MnO	NiO	CaO	Total
000b	40.62	0.02	0.01	8.54	50.02	0.04	0.28	0.00	99.53
001a	40.38	0.00	0.06	8.21	50.45	0.02	0.35	0.00	99.47
002a	40.99	0.00	0.04	8.49	50.64	0.09	0.31	0.05	100.56
004c	40.50	0.00	0.01	8.31	50.07	0.08	0.33	0.00	99.30
005a	40.11	0.00	0.00	7.91	50.48	0.03	0.47	0.00	99.00
006b	40.16	0.00	0.05	9.16	49.48	0.10	0.43	0.05	99.38
012a	40.84	0.00	0.02	8.15	50.57	0.06	0.30	0.00	99.58
014b	40.58	0.01	0.04	9.84	49.15	0.11	0.43	0.06	100.22
021a	40.42	0.00	0.06	8.16	50.36	0.05	0.40	0.00	99.45
031b	40.45	0.02	0.02	8.68	49.61	0.09	0.30	0.00	99.17
032c	40.12	0.00	0.00	7.78	50.86	0.05	0.54	0.00	99.35
036b	40.64	0.02	0.04	8.18	50.26	0.11	0.34	0.00	99.59
041c	40.23	0.00	0.02	9.23	49.46	0.08	0.35	0.00	99.37
045c	40.30	0.00	0.00	9.39	49.30	0.06	0.40	0.01	99.38
046c	40.08	0.00	0.03	8.51	50.12	0.06	0.40	0.00	99.20
048c	40.45	0.00	0.00	7.81	50.45	0.07	0.33	0.00	99.11
055c	40.49	0.00	0.06	8.04	50.14	0.05	0.33	0.00	99.11
056b	40.40	0.00	0.03	7.70	50.95	0.11	0.43	0.01	99.63
057b	40.70	0.00	0.02	8.09	50.47	0.02	0.33	0.00	99.63
059b	40.63	0.00	0.08	80.2	50.29	0.11	0.30	0.02	99.45

TABLE 1b. AVERAGE COMPOSITION OF OLIVINE IN HAM SPINEL LHERZOLITE

#	SiO_2	TiO_2	Cr_2O_3	FeO*	MgO	MnO	NiO	CaO	Total
051a	40.40	0.02	0.08	7.83	50.71	0.04	0.39	0.00	99.47
071a	40.54	0.00	0.00	7.79	50.85	0.08	0.39	0.00	99.65

* total iron as FeO. a Granular, b porphyroclastic, c mosaic.

Olivine in spinel lherzolite is magnesium- and nickel-rich ($Fo_{91.9}$–$Fo_{92.2}$, 0.30–0.48 wt.% NiO), with forsterite contents falling within the compositional range of olivine in granular garnet lherzolites.

Orthopyroxene

Compositionally (Table 2), orthopyroxene is a Cr–Al-poor enstatite [100 Mg/(Mg + Fe) 91.4-93.5]. Negligible compositional variation was detected within each population in the garnet lherzolite xenoliths, although significant intergrain compositional differences were detected in spinel lherzolite xenoliths. The compositional variation in general parallels textural changes in the xenolith suite, orthopyroxene in mosaic-textured xenoliths being iron- and calcium-rich [100 Mg/(Mg + Fe) 0.914 to 0.925, 0.90 to 1.10 wt.% CaO] and chrome-poor (0.30 to 0.50 wt.% Cr_2O_3) compared to orthopyroxene in porphyroclastic [100 Mg/(Mg + Fe) 92.2 to 93.2, 0.75 to 0.95 wt.% CaO, 0.30 to 0.65 wt.% Cr_2O_3] and granular-textured xenoliths [100 Mg/(Mg + Fe) 92.8 to 93.5, 0.60 to 0.92 wt. % CaO, 0.30 to 0.75 wt.% Cr_2O_3]. Aluminum is weakly enriched in mosaic-textured xenoliths compared to porphyroclastic and granular types, the former on average containing 1.27 wt.% Al_2O_3, and the latter types, which cannot be distinguished chemically, containing on average 1.09 wt.% Al_2O_3.

Orthopyroxene in the two xenoliths of spinel lherzolite (Ham 051 and 071) are compositionally simi-

TABLE 2a. AVERAGE COMPOSITION OF ORTHOPYROXENE FROM HAM GARNET LHERZOLITE

#	SiO_2	TiO_2	Al_2O_3	Cr_2O_3	FeO*	MgO	MnO	NiO	CaO	Total
000b	56.51	0.08	1.15	0.36	5.09	35.70	0.03	0.02	0.83	99.87
001a	56.56	0.13	1.40	0.59	4.75	35.70	0.09	0.00	0.89	100.11
002a	57.39	0.13	1.08	0.45	5.12	34.77	0.13	0.05	0.61	99.73
004c	56.08	0.19	1.14	0.45	4.99	35.83	0.06	0.07	0.78	99.59
005a	56.13	0.21	1.11	0.49	4.90	36.23	0.03	0.00	0.77	99.87
006b	55.71	0.14	1.24	0.36	5.86	35.98	0.05	0.03	1.03	100.40
012a	56.60	0.00	1.13	0.70	4.93	36.23	0.04	0.09	0.78	100.50
014b	57.12	0.23	1.48	0.40	6.40	33.90	0.08	0.06	1.13	100.80
021a	56.54	0.00	1.09	0.33	4.86	36.09	0.04	0 06	0.67	99.68
031b	56.10	0.06	1.28	0.32	5.22	35.50	0.05	0.09	0.82	99.44
032c	56.69	0.02	0.90	0.39	4.88	36.79	0.04	0.04	0.41	100.15
036b	56.61	0.01	1.09	0.54	4.84	36.12	0.05	0.06	0.72	100.40
041c	55.97	0.24	1.14	0.50	5.58	35.10	0.06	0.07	0.98	99.64
045c	56.29	0.00	1.45	0.37	5.60	34.98	0.07	0.07	1.05	99.88
046c	56.08	0.21	1.23	0.52	5.27	35.58	0.04	0.14	0.96	100.30
048c	56.58	0.03	1.11	0.59	4.76	36.20	0.06	0.07	0.79	100.19
055c	56.37	0.13	1.20	0.52	4.87	36.14	0.06	0.09	0.89	100.27
056b	56.42	0.00	1.06	0.59	4.64	36.44	0.04	0.09	0.70	99.98
057b	57.34	0.00	1.16	0.47	4.79	35.92	0.01	0.05	0.87	100.61
059b	56.40	0.00	1.19	0.48	4.85	35.94	0.02	0.08	0.90	99.86

TABLE 2b. AVERAGE COMPOSITION OF ORTHOPYROXENE FROM HAM SPINEL LHERZOLITE

#	SiO_2	TiO_2	Al_2O_3	Cr_2O_3	FeO*	MgO	MnO	NiO	CaO	Total
051a	56.70	0.03	0.94	0.67	4.90	36.36	0.03	0.06	0.52	100.21
071a	56.23	0.01	2.27	0.36	5.26	36.07	0.09	0.00	0.25	100.54

* total iron as FeO. a Granular, b porphyroclastic, c mosaic.

TABLE 3a. AVERAGE COMPOSITION OF CLINOPYROXENE FROM HAM GARNET LHERZOLITE

#	SiO_2	TiO_2	Al_2O_3	Cr_2O_3	FeO*	MgO	MnO	CaO	Na_2O	Total
000b	55.47	0.22	2.45	1.42	2.22	17.72	0.00	19.39	1.46	100.35
001a	55.14	0.26	2.56	1.89	2.38	17.62	0.00	18.42	1.65	99.92
002a	54.30	0.28	2.51	1.75	2.51	16.98	0.09	18.80	1.92	99.16
004c	54.78	0.55	2.30	1.37	2.52	17.94	0.00	19.01	1.43	99.90
005a	55.37	0.31	2.20	1.84	2.39	17.87	0.00	19.03	1.41	100.42
006b	54.99	0.28	2.19	1.40	3.27	18.27	0.00	18.01	1.16	99.57
012a	54.97	0.00	1.73	2.37	2.36	17.60	0.00	18.97	1.29	99.29
014b	54.10	0.45	2.53	1.20	3.60	18.33	0.13	17.68	1.43	99.45
021a	55.35	0.10	2.47	1.56	2.51	17.44	0.00	18.97	1.60	100.00
031b	55.10	0.27	2.45	1.40	2.77	17.40	0.00	18.62	1.49	99.50
032c	55.22	0.10	2.28	1.90	1.88	16.44	0.00	20.76	1.68	100.26
036b	55.36	0.10	1.87	1.97	2.38	17.98	0.00	19.62	1.26	100.54
041c	54.88	0.67	2.01	1.50	2.84	18.30	0.00	18.76	1.18	100.14
045c	55.41	0.06	2.31	1.11	2.78	18.63	0.01	18.76	1.12	100.19
046c	55.36	0.38	1.76	1.22	2.84	18.44	0.00	19.10	0.88	99.98
048c	55.32	0.10	1.96	1.68	2.42	18.07	0.00	19.33	1.24	100.12
055c	54.77	0.40	2.21	1.70	2.58	17.84	0.00	18.56	1.38	99.44
056b	55.01	0.04	1.81	2.21	1.99	17.47	0.00	20.06	1.29	99.88
057b	55.39	0.10	1.95	1.54	2.62	18.52	0.00	19.28	1.12	100.52
059b	54.98	0.16	1.87	1.54	2.52	18.44	0.01	18.94	1.07	99.53

TABLE 3b. AVERAGE COMPOSITION OF CLINOPYROXENE FROM HAM SPINEL LHERZOLITE

#	SiO_2	TiO_2	Al_2O_3	Cr_2O_3	FeO*	MgO	MnO	CaO	Na_2O	Total
051a	55.35	0.24	2.20	3.13	2.21	16.61	0.00	18.51	2.02	100.27
071a	54.12	0.06	3.93	1.22	1.56	16.09	0.00	21.21	1.22	99.41

* total iron as FeO. a Granular, b porphyroclastic, c mosaic.

lar, the former being only slightly magnesium-rich but significantly calcium-rich [av. 100 Mg/(Mg + Fe) 92.9, av. 0.52 wt.% CaO] compared to the latter [av. 100 Mg/(Mg + Fe) 92.4, av. 0.24 wt.% CaO]. Alumina and chrome contents in Ham 051 have restricted compositional ranges (0.80 to 0.98 wt.% Al_2O_3, 0.58 to 0.70 wt.% Cr_2O_3) compared to the Ham 071, in which alumina and chrome vary widely (0.54 to 3.20 wt.% Al_2O_3, 0 to 0.58 wt.% Cr_2O_3). The broad compositional range displayed by orthopyroxene and clinopyroxene (see below) in Ham 071 suggests that this xenolith contains a disequilibrium assemblage of minerals.

Clinopyroxene

Clinopyroxene in all xenoliths of garnet lherzolite except Ham 032 is compositionally uniform (Table 3). That in mosaic-textured xenoliths is slightly calcium-poor [Ca/(Ca + Mg) 0.415 to 0.430] and has a broader range in titanium content (0 to 0.83 wt.% TiO_2) compared to compositionally similar pyroxene in porphyroclastic- and granular-textured xenoliths [Ca/(Ca + Mg) 0.425 to 0.455, 0 to 0.41 wt.% TiO_2]. The aluminum and sodium content of all pyroxenes is similar. The pyroxene in Ham 032 is distinctly calcium-rich and magnesium-poor [Ca/(Ca + Mg) 0.472 to 0.495] compared to that in other garnet lherzolite xenoliths [Ca/(Ca + Mg) 0.415 to 0.455]. It is intermediate in composition between the latter and clinopyroxene in spinel lherzolite 071.

The compositions of clinopyroxene in spinel lherzolite demonstrate a bimodal variation both within and between the two xenoliths. The light green clinopyroxene in Ham 051 is compositionally similar to clinopyroxene in garnet lherzolite in that it has comparable Ti (0.10 to 0.40 wt.% TiO_2) and Al contents (1.90 to 2.41 wt.% Al_2O_3) and a slightly higher Na content (1.66 to 2.33 wt.%). The core of a single dark green clinopyroxene is distinctly magnesium-rich [Ca/(Ca + Mg) 0.399] compared to the rim (turbid, light green) [Ca/(Ca + Mg) 0.441] and to other pyroxene grains in the same xenolith. The crystallization of tiny euhedral grains of aluminous magnesian chromite (see below) in an alteration mantle around this grain accounts for the depletion of minor elements in the rim of the pyroxene relative to the core (rim–core TiO_2 0.11 *versus* 0.28 wt.%, Al_2O_3 1.91 *versus* 2.27 wt.%, Cr_2O_3 2.79 *versus* 2.96 wt.%, FeO 2.29 *versus* 2.65 wt.%). These spinel grains are compositionally similar to larger lobate grains associated with Ca-rich pyroxene elsewhere in the xenolith.

The pyroxene in Ham 071 demonstrates a bimodal compositional variation, both the calcium-poor [Ca/(Ca + Mg) 0.441] and calcium-rich [Ca/(Ca + Mg) 0.505 to 0.515] varieties containing an average lower Ti (0 to 0.25 wt.% TiO_2) and higher Al (3.55 to 4.39 wt.% Al_2O_3) contents than pyroxene in other spinel and garnet lherzolite xenoliths. This bimodal compositional variation reflects the disequilibrium nature of this lherzolite assemblage.

Garnet

The garnet in the xenoliths is chrome-pyrope (Group 9 of Dawson & Stephens 1975; Table 4). Ti-poor and unusually Ti-rich varieties are present. Iron-rich types are absent. The compositions of the garnet in all xenoliths span a similar range of Mg/(Mg + Ca), 0.824 to 0.872, those from granular-textured xenoliths demonstrating the broadest range and those from mosaic-textured xenoliths containing on average the highest Fe/(Fe + Mg) [av. Fe/(Fe + Mg) 0.153] values. Two mosaic-textured xenoliths (Ham 041, 046) contain unusually Ti-rich garnet (0.41 to 0.71 wt.% TiO_2, 5.25 to 5.80 wt.% Cr_2O_3) and are weakly iron- and calcium-rich compared to the relatively Ti-poor garnet (TiO_2 < 0.40 wt.%) in granular-, porphyroclastic- and other mosaic-textured xenoliths. Detailed microprobe traverses were not attempted across individual grains, so that the presence of complex patterns of zoning, such as those detected in Ti-rich metasomatic garnet by Smith & Ehrenberg (1984) and Laz'ko & Serenko (1984), could not be detected.

TABLE 4. AVERAGE COMPOSITION OF GARNET FROM HAM GARNET LHERZOLITE

#	SiO_2	TiO_2	Al_2O_3	Cr_2O_3	FeO*	MgO	MnO	CaO	Total
000b	41.59	0.33	20.79	3.45	6.74	21.99	0.28	4.91	100.08
001a	41.33	0.35	19.71	5.00	6.14	22.21	0.23	4.91	99.88
002a	42.18	0.29	20.99	3.87	7.40	21.07	0.39	4.85	101.14
004c	41.57	0.30	20.42	3.93	6.52	21.90	0.16	5.13	99.93
005a	41.37	0.18	20.19	4.45	6.39	22.09	0.23	5.04	99.94
006b	41.14	0.32	19.66	4.49	7.06	21.44	0.13	5.43	99.67
012a	41.05	0.00	17.65	8.57	6.39	20.82	0.29	6.17	100.94
014b	41.28	0.51	20.11	4.03	7.34	20.34	0.34	5.36	99.30
021a	41.87	0.05	21.44	3.21	6.61	22.42	0.24	4.67	100.51
031b	41.51	0.26	20.63	3.09	7.05	22.32	0.20	4.57	99.63
032c	41.46	0.04	20.74	4.01	7.01	21.19	0.32	4.99	99.76
036b	40.98	0.00	18.71	6.72	6.39	21.28	0.26	5.59	99.93
041c	40.80	0.87	18.67	5.35	7.23	21.04	0.23	5.85	100.04
045c	41.61	0.08	20.90	3.45	6.95	21.85	0.17	5.19	100.20
046c	40.75	0.56	19.00	5.64	6.74	21.09	0.24	6.05	100.07
048c	41.67	0.16	19.55	5.31	6.06	21.83	0.24	5.41	100.23
055c	41.05	0.25	19.07	5.83	6.05	21.88	0.17	5.27	99.57
056b	41.00	0.09	18.43	7.10	6.25	21.13	0.28	5.86	100.14
057b	42.93	0.06	18.71	6.24	6.26	20.93	0.14	5.54	100.81
059b	41.41	0.15	19.40	5.66	6.22	21.54	0.19	5.76	100.33

*Total iron as FeO. a Granular, b porphyroclastic, c mosaic.

Spinel

Two compositionally distinct spinels (Table 5) occur in the spinel lherzolites. Ham 051 contains Ti-rich (av. 4.62 wt.% TiO_2) aluminous magnesian chromite [av. Cr/(Cr + Al) 0.778, av. Fe/(Fe + Mg) 0.419] both as an intergranular phase and as tiny euhedral grains [3.85 wt.% TiO_2, Cr/(Cr + Al) 0.777, Fe/(Fe + Mg) 0.399] in the recrystallized margin of a compositionally zoned clinopyroxene grain. Coexisting orthopyroxene has an average Al_2O_3 content of 0.94 wt.%. This xenolith, according to Carswell's (1980) classification, is a chromite lherzolite.

The spinel in Ham 071 (Table 5) is a compositionally uniform Fe-rich member of the chromite-pleonaste series [av. Cr/(Cr + Al) 0.309, av. Fe/(Fe + Mg) 0.305]. Using Carswell's classification scheme, Ham 071 is a Cr-spinel lherzolite, the spinel coexisting with a relatively aluminum-rich orthopyroxene (1.89 wt.% Al_2O_3).

TABLE 5. AVERAGE COMPOSITION OF SPINEL IN HAM SPINEL LHERZOLITE

#	SiO_2	TiO_2	Al_2O_3	Cr_2O_3	FeO*	MnO	MgO	NiO	Total
051a	-	4.62	10.09	51.65	19.16	0.40	14.90	0.19	101.01
051b	1.01	3.85	9.52	51.15	18.96	0.42	15.45	0.21	100.57
071	-	0.04	40.61	27.05	13.86	0.37	17.88	0.17	99.98

051a - ovoid, opaque spinel

051b - subhedral to euhedral, opaque spinel found in the reaction margin of a highly altered, bright-green chrome-diopside.

071 - translucent, orange-red, cuspate spinel.

TABLE 6. COMPOSITION OF ROUND INCLUSIONS AND COLLARS ON MINERAL GRAINS IN LHERZOLITE MINERALS

A
Olivine

#	SiO_2	TiO_2	Al_2O_3	Cr_2O_3	FeO*	MgO	MnO	NiO	CaO	Total
001	40.40	0.00	0.00	0.18	8.15	50.53	0.00	0.38	0.00	99.69
004	40.51	0.00	0.00	0.07	8.08	50.02	0.10	0.29	0.00	99.07
036	40.73	0.00	0.00	0.00	8.10	50.55	0.16	0.35	0.00	100.00
036	40.79	0.08	0.00	0.05	8.26	50.22	0.00	0.26	0.00	99.73
051	40.48	0.00	0.00	0.15	7.73	50.58	0.00	0.37	0.00	99.41
055*	40.42	0.00	0.00	0.00	8.16	49.96	0.06	0.35	0.00	99.01
059	40.69	0.00	0.00	0.05	8.00	50.31	0.09	0.30	0.05	99.49
059**	40.80	0.00	0.00	0.07	8.02	50.41	0.08	0.33	0.00	99.75

All examples included in garnet except (*) in garnet kelyphite and (**) in orthopyroxene.

B
Clinopyroxene

#	SiO_2	TiO_2	Al_2O_3	Cr_2O_3	FeO*	MgO	CaO	MnO	NiO	Na_2O	Total
21a	55.58	0.07	2.42	1.41	2.38	17.37	19.20	0.00	0.00	1.65	100.07
21b*	55.37	0.07	2.45	1.54	2.46	17.33	19.34	0.00	0.00	1.56	100.12
21c*	54.95	0.00	2.30	1.38	2.58	17.19	19.14	0.00	0.00	1.41	98.95
45	55.19	0.10	2.34	1.16	2.81	18.61	18.58	0.00	0.00	1.04	99.82
57**	55.50	0.21	1.89	1.42	2.66	18.42	19.64	0.00	0.00	1.04	100.91

All examples included in garnet except (*) which represents a discontinuous collar around a garnet and (**) an inclusion in olivine.

C
Orthopyroxene**

#	SiO_2	TiO_2	Al_2O_3	Cr_2O_3	FeO*	MgO	MnO	NiO	CaO	Total
55	55.58	0.00	1.11	0.38	5.00	36.80	0.00	0.00	0.77	99.64

**Grain included in an olivine.

* Total iron as FeO.

Silicate inclusions

A comparison of Table 6 and Tables 1 to 3 shows that mineral inclusions are similar in composition to the average composition of that mineral species in the xenolith framework. Smith & Ehrenberg (1984) determined a similar relationship for olivine, orthopyroxene and clinopyroxene that occur as inclusions in metasomatized xenoliths, but showed that garnet as inclusions differs compositionally from the framework garnet. They concluded that this difference is due to slower rates of cation diffusion and chemical equilibration between the included garnet

TABLE 7. EQUILIBRATION TEMPERATURES AND PRESSURES OF XENOLITHS

Garnet lherzolite		Temperature °C						Pressure kbars		
		A	B	C	D	E	F	1	2	3
000	b	1067	1098	1107	1170	1093	1318	37.3	40.1	45.2
001	a	1094	1148	1134	1196	1199	1379	36.1	40.1	45.4
002	a	1022	1084	1089	1057	1117	1057	35.5	40.3	45.2
004	c	1085	1136	1126	1169	1198	1331	38.3	42.6	47.6
005	a	1080	1130	1118	1155	1156	1251	38.4	43.4	47.6
006	b	1151	1204	1209	1283	1308	1321	40.2	43.0	50.7
012	a	1093	1113	1134	1114	1178	1263	37.5	39.4	46.5
014	b	1141	1221	1284	1207	1293	1297	36.7	40.1	49.0
021	a	1064	1104	1100	1195	1211	1293	38.3	42.1	46.4
031	b	1087	1121	1131	1220	1217	1255	37.3	40.0	45.2
032	c	927	855	947	970	1017	1037	32.5	30.1	33.3
036	b	1076	1099	1114	1121	1169	1271	37.8	39.9	46.1
041	c	1126	1167	1180	1138	1187	1297	39.5	42.4	49.7
045	c	1137	1183	1193	1165	1174	1414	37.4	40.7	47.7
046	c	1140	1156	1192	1185	1234	1249	38.9	40.5	47.9
048	c	1093	1123	1132	1186	1225	1349	38.8	42.7	47.3
055	c	1109	1152	1151	1250	1274	1380	38.3	41.7	48.0
056	b	1038	1032	1069	1033	1092	1214	35.7	36.5	42.4
057	b	1113	1150	1156	1171	1217	1280	39.1	38.7	48.5
059	b	1120	1165	1164	1172	1216	1310	38.8	41.6	48.9
Spinel lherzolite										
		A	G	H						
051		1062	435	272	(framework-framework cpx-opx)					
051		1141	-	-	(core-framework cpx-opx)					
051		1059	458	295	(rim-framework cpx-opx)					
071		950	929	251						

a Granular, b porphyroclastic, c mosaic. Temperatures from A) Wells (1977) pyroxene solvus, B) Finnerty & Boyd (1987) pyroxene solvus, C) Mori & Green (1978) pyroxene solvus, D) Mori & Green (1978) K_D garnet - clinopyroxene, E) Ellis & Green (1979) K_D garnet - clinopyroxene, F) O'Neill & Wood (1979) garnet - olivine equilibria, G) Fabriès (1979) spinel - olivine equilibria, H) Roeder *et al.* (1979) spinel - olivine equilibria. Pressures from 1) Wells (1977) - Wood (1974), no correction for Cr, 2) Finnerty & Boyd (1987) - Wood (1974), no correction for Cr, 3) Finnerty & Boyd (1987) - MacGregor (1974).

and its host compared to olivine and pyroxene. The single crystal of garnet found as an included phase in the Ham xenoliths was not analyzed, so that this interpretation was not tested.

GEOTHERMOBAROMETRY

Table 7 presents estimates of equilibration temperatures and pressures of garnet and spinel lherzolites calculated using the pyroxene solvus (Wells 1977, Finnerty & Boyd 1987, Mori & Green 1978), garnet–clinopyroxene (Mori & Green 1978, Ellis & Green 1979) and spinel–olivine equilibria (Fabriès 1979, Roeder *et al.* 1979).

The Wells (1977) formulation of the pyroxene solvus consistently estimates lower temperatures than all the other methods. The discrepancies among the calculated temperatures are not consistent among methods and do not increase with increasing temperature. Temperature differences are not a function of textural type, nor of contents of iron and minor elements, as observed by Carswell & Gibb (1980).

Carswell & Gibb (1980) indicated that a mean temperature calculated by their five recommended methods (Table 7) is suitable as an estimate of temperature if there is good agreement among the methods. Mitchell (1984), however, contended that this approach is unreasonable if there is a wide range in the calculated temperatures and suggested that the mean temperature is no more valid than one determined by any single method. The wide range in calculated temperatures given in Table 7 thus suggests that a single calculation is more appropriate for the Ham data than the averaging method used by Carswell & Gibb (1980).

Temperatures calculated by the methods of Finnerty & Boyd (1987) and Mori & Green (1978) are in good agreement in general. The Finnerty & Boyd (1987) approach is based upon new reversed experimental studies of the pyroxene solvus by Nickel & Brey (1984) and Brey & Huth (1984) at high pressures. Typically, temperatures calculated by this method are up to 50°C higher than temperatures calculated using the approach of Wells (1977).

As yet there is no agreement as to which of the geothermometers available gives accurate estimates of equilibration temperatures. Carswell (1980) and Mitchell *et al.* (1980) have suggested that the method of Wells (1977) gives the closest agreement between calculated temperatures and measured temperatures for natural assemblages equilibrated at known temperatures and pressures. Finnerty & Boyd (1984, 1987) have argued, however, that only geothermobarometers that place graphite- or diamond-bearing lherzolites in their correct fields of stability relative to the diamond–graphite univariant curve are reliable. Finnerty & Boyd (1987) claim that only the Lindsley & Dixon (1976) 20-kbar solvus and their new formulation of the solvus meet these constraints. Discussion of the relative merits of the various geothermometers is beyond the scope of this paper. Temperatures based on the Wells (1977) method have been used here to calculate equilibration pressures in order that direct comparison may be made with the previously published equilibration-parameters of Somerset Island lherzolites (Mitchell 1978).

Pressures of equilibration for the garnet lherzolites are thus calculated using the Wells (1977) temperatures in conjunction with Wood's (1974) formulation of MacGregor's (1975) data for the incorporation of aluminum in orthopyroxene coexisting with garnet. Corrections for chromium content have not been applied to the data, as Mitchell *et al.* (1980) showed that such a correction introduces unwarranted discrepancies into calculated pressures compared to calculations that neglect the influence of chromium.

Table 7 thus shows that the garnet lherzolites from Ham have equilibrated at 927–1151°C over a pressure range of 32 to 40 kbar. No simple relationship exists between textural type and equilibration temperatures. Coarse-textured (1022–1094°C, 35.5–38.4

kbar), porphyroclastic-textured (1038–1151°C, 35.7–40.2 kbar) and mosaic-textured (1085–1140°C, 37.4–39.5 kbar) xenoliths, with the exception of Ham 032 (mosaic-porphyroclastic), have equilibrated over similar relatively limited intervals of temperature and pressure. Although mosaic-textured xenoliths in general give the highest temperatures of equilibration, Ham 032 has equilibrated to the lowest temperature (927°C) and pressure (32.5 kbar) found for this xenolith suite.

Figure 1 depicts the temperature–pressure array of equilibration data for the Ham xenoliths in relation to several theoretical shield-geotherms (Gurney & Harte 1980) and to the graphite–diamond univariant curve (Kennedy & Kennedy 1976). The data points do not define a curvilinear array that could be interpreted as a geotherm but form a diffuse cluster approximately coincident with a 44-mWm^{-2} theoretical shield-geotherm and with the upper limb of an apparent geotherm defined by other garnet lherzolite data from Somerset Island (Mitchell 1978, 1987). Ham 032, a low-temperature mosaic-porphyroclastic-textured xenolith, plots with several low-temperature coarse lherzolites from Somerset Island (Mitchell 1978) close to the 44-mWm^{-2} geotherm. Mitchell (1978) interpreted these data as defining the lower limb of an inflected geotherm. However, the paucity of such low-temperature xenoliths from the Ham kimberlite precludes further interpretation of the data.

Together, all the data for the Somerset Island garnet lherzolite suite define an inflected or perturbed geotherm, in which the majority of samples regardless of textural type plot at relatively high temperatures over a limited range of pressure (Fig. 1). All of the Somerset Island data have equilibration parameters outside the stability field of diamond.

Apparent geotherms of similar configuration and orientation with respect to theoretical geotherms and the diamond–graphite univariant curve have been described from Namibia (Mitchell 1984) and East Griqualand (Nixon & Boyd 1979). A similar lack of correlation between equilibration temperature and textural type has been noted for xenoliths derived from Namibia (Mitchell 1984), Matsoku (Harte *et al.* 1975) and the Kimberley area (Boyd & Nixon 1978).

Equilibration temperatures of clinopyroxene-bearing spinel lherzolite xenoliths may be calculated using two methods. Owing to uncertainties in thermodynamic data for spinels, the pyroxene solvus geothermometer (Wells 1977) is considered to give more reliable estimates of temperature than methods based upon Irvine's (1965) olivine–spinel geothermometer. Fabriès (1979) and Roeder *et al.* (1979) have demonstrated that the latter method can give realistic temperatures if applied to rapidly transported mantle-derived assemblages. However, application to Alpine and basic intrusive complexes demonstrates that re-equilibration to low tempera-

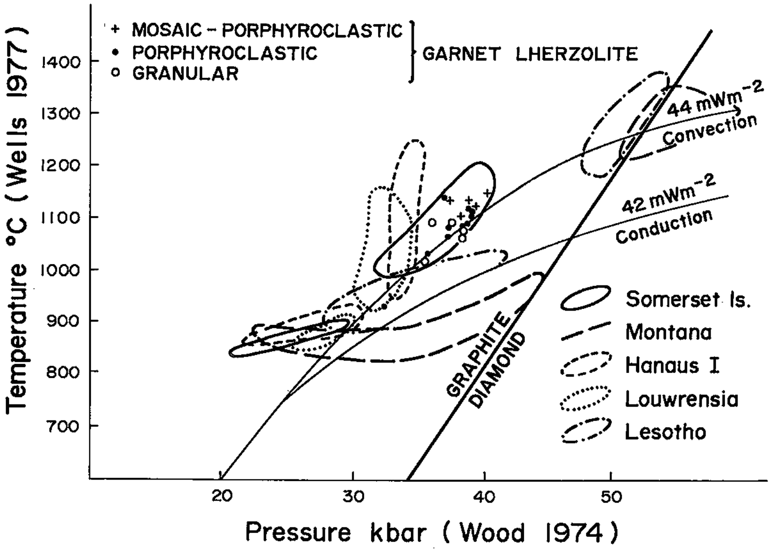

FIG. 1. Equilibration conditions of the Ham garnet lherzolite xenoliths. Data for Lesotho, Montana, Namibia, East Griqualand and Somerset Island from Nixon & Boyd (1973), Hearne & McGee (1984), Mitchell (1984), Nixon & Boyd (1979) and Mitchell (1978), Mitchell *et al.* (1980), respectively. Representative shield-geotherms of 44 mWm^{-2} (convection) and 42 mWm^{-2} (conduction) are from Gurney & Harte (1980).

tures easily occurs during slow cooling in the upper crust.

According to geothermometry based on the pyroxene solvus (Wells 1977), the spinel lherzolites have equilibrated between 950 and 1142°C. Ham 071, a Cr-spinel lherzolite, gives the lowest temperature (950°C), and Ham 051, a chromite lherzolite with a disequilibrium assemblage, a range of temperatures. Framework pyroxenes in the latter have equilibrated at 1062°C, in contrast to the high temperature (1142°C) calculated for the core of a non-equilibrium clinopyroxene and framework orthopyroxene. The equilibration temperature for the rim assemblage (1059°C), which contains euhedral chromite that is compositionally similar to the framework chromite, is in close agreement with the temperature calculated for the framework pyroxenes (1062°C).

Spinel–olivine equilibration temperatures (Table 7) calculated using either the Fabriès (1979) or Roeder *et al.* (1979) methods are at variance with the pyroxene solvus temperatures. These discrepancies suggest the presence of a disequilibrium assemblage.

Pressures of equilibration of the spinel lherzolites may be crudely estimated using temperatures derived by the method of Wells (1977) in conjunction with experimental data presented by Obata (1980) and O'Hara *et al.* (1971), for the stability of spinel, garnet–spinel, and garnet lherzolites. Temperatures and pressures of equilibration for the core of a disequilibrium clinopyroxene in Ham 051 suggest that this xenolith originally equilibrated at approximately 1142°C and 19–20 kbar pressure. Equilibration parameters for the framework minerals indicate partial re-equilibration at approximately 1060°C at 17–18 kbar. Ham 071 equilibrated at 950°C at 16–17 kbar.

The data on spinel lherzolite equilibration are consistent with derivation of these xenoliths from high levels of the upper mantle, together with re-equilibration of the olivine and spinels during transport and cooling in their kimberlite host.

DISCUSSION

A lack of correlation between increasing temperature and intensity of deformation in lherzolite xenoliths with increasing depth has been recognized in some Canadian (Mitchell 1978, 1987) and South African suites of xenoliths (Dawson 1981, Mitchell 1984). This relationship conflicts with Boyd's (1973) model, which is based upon stress-related heating and deformation associated with lateral movements at the lithosphere–asthenosphere boundary. Boyd (1973) and Boyd & Nixon (1975, 1978) proposed that the porphyroclastic- and mosaic-textured xenoliths that comprise the inflected limb of mantle geotherms formed at this boundary; however, Goetze (1975) argued that annealing would recrystallize deformation fabrics in such a pressure–temperature regime. The model of Green & Gueguen (1974), later developed by Mitchell (1978, 1984), Mitchell *et al.* (1980) and Gurney & Harte (1980), proposes that these textures were formed at higher levels in the mantle, around an ascending diapir. Deformation fabrics would escape the effects of annealing owing to their rapid transport in an ascending kimberlite magma. Mitchell (1984) argued that although the lower limb of an inflected mantle geotherm may reflect the steady-state mantle geotherm, the inflected high-temperature limb is generated in response to a thermal gradient about the rising diapir. In this manner, a transient apparent geotherm is formed in response to the thermal (Mitchell 1984) and possibly metasomatic effects (Gurney & Harte 1980) of a rising diapir.

Mitchell (1984) proposed that the population of mantle-derived xenoliths possibly can contain xenoliths from at least three mantle sources. These include restite or residual mantle, representing fragments of the upwelling diapir, modified mantle representing material from the thermal aureole (which may or may not be metasomatized), and unmodified xenoliths that represent mantle material derived from outside the area of influence of the diapir's thermal aureole. Owing to the slow ascent of the diapir, Mitchell (1984) contended that continual re-equilibration of xenoliths may occur and that the maximum temperatures and pressures of equilibration may represent the minimum temperature and depth of magma separation from the source lithology. These xenoliths do not retain any evidence of their high-pressure and high-temperature source region and may give equilibration temperatures similar to modified xenoliths.

Restite and modified xenoliths, therefore, do not retain information regarding the steady-state thermal structure of their source region and are regarded as comprizing the inflected limb of mantle geotherms (*e.g.*, Mitchell 1984). Unmodified xenoliths that have escaped the thermal and metasomatic effects of the rising diapir will preserve steady-state thermostratigraphic evidence and, therefore, form the lower limb of a perturbed geotherm.

The xenolith population at Ham comprises both high- and low-temperature, coarse and highly deformed xenoliths. Such a mixed suite cannot be entirely explained using models proposed by Boyd (1973), Boyd & Nixon (1975, 1978) or Mitchell (1984). The following model suggesting lateral and vertical structural inhomogeneities in the mantle about a magma source is proposed to account in part for the range of deformation fabrics in the suite of xenoliths.

It is reasonable to assume that a temperature gradient will form around an ascending heat-source. The heat source may be associated with rising hot volatiles from deeper portions of the mantle or with an ascending diapir. At any given time, if upward migration is slow enough, isotherms will decrease in a semiconcentric manner away from the source. This temperature gradient may be equated to the inflected limb of perturbed geotherms and, at shallower levels in the mantle, will intersect the steady-state mantle geotherm (Green & Gueguen 1974). Deformation fabrics and fracture propagation may not be associated directly with an ascending diapir, but may be initiated by partial melting upon pressure release, promoted by the infiltration of hot metasomatic fluids (Spera 1981) to the levels that are stratigraphically higher than the diapir. Thus as fusion progresses and the volume of magma produced by partial melting increases, the magma pressure within the partial melt region may gradually rise above the mean normal stress due to lithostatic load. Spence & Turcotte (1985) showed that long cracks (1 to 10^2 km) of narrow width (0.1 to 5 m) will occur when driven by a slightly pressurized magma. Spera (1984) indicated that fracture-swarm propagation also is a plausible consequence of overpressure failure. Ductile shear, as evidenced by mosaic and porphyroclastic textures, is a likely mechanism of failure. In a high-pressure and high-temperature regime, such fabrics may be laterally zoned about planes of failure, so that mosaic-textured mantle would occur at the core and grade outward ultimately into granular textures. In an anastomozing swarm of fractures, "islands" of undeformed mantle could be surrounded by highly deformed mantle. Such zonation in fabrics has been recorded by Dawson *et al.* (1975). Importantly, the lateral zonation would not record a temperature gradient, as the range of fabrics would be developed at the same thermobarometric horizon in the mantle. Thus as a kimberlite magma ascends through these fractures and begins to entrain mantle material, it will initially sample highly deformed mantle and gradually, through attrition of the conduit walls, incorporate progressively less-deformed mantle. In regions where "islands" of undeformed mantle occur, successive batches of magma could sample mantle with a wide range of textures.

This isothermal lateral zonation may be expected to occur at any level in the mantle above the magma source. However, vertical zonation in fabric and a decrease in the width of the deformation halo also may occur at shallower depths if the intensity of volatile-induced fracturing decreases with decreasing depth. It follows that kimberlite magmas derived from relatively immature source-regions may contain a xenolith population with thermotextural characteristics similar to those described by Boyd (1973) and Boyd & Nixon (1975, 1978). In contrast, mature areas may yield a population of xenoliths containing both high-temperature granular- and mosaic-textured xenoliths. These relationships can be complicated further by multiple episodes of magmatism, batch mixing of magmas, the rheological sorting and attrition of xenoliths in rapidly ascending magmas and, possibly, metasomatically induced temperature-gradients developed about fluid conduits.

ACKNOWLEDGEMENTS

This study was supported in the field in part by the Polar Continental Shelf Project and financially by the Natural Sciences and Engineering Research Council of Canada. Bruce Jago thanks the Senate Research Committee at Lakehead University for generously allocating travel funds to conduct this research. Barry Clarke is thanked for access to the microprobe facilities at Dalhousie University, and Valerie Dennison is thanked for field assistance. Tony Carswell and Joe Boyd are thanked for the use of the NODMINS and TEMPEST programs, respectively, used for the calculation of equilibration parameters.

REFERENCES

BOYD, F.R. (1973): A pyroxene geotherm. *Geochim. Cosmochim. Acta* **37**, 2533-2546.

______ & FINGER, L.W. (1975): Homogeneity of minerals in mantle rocks from Lesotho. *Carnegie Inst. Wash. Year Book* **74**, 519-525.

______ & NIXON, P.H. (1975): Origins of ultramafic nodules from some kimberlites of northern Lesotho and the Monastery mine, South Africa. *Phys. Chem. Earth* **9**, 431-454.

______ & ______ (1978): Ultramafic nodules from the Kimberley pipes, South Africa. *Geochim. Cosmochim. Acta* **42**, 1367-1382.

BREY, G. & HUTH, J. (1984): The enstatite–diopside solvus to 60 kbar. *In* Kimberlites II: The Mantle and Crust-Mantle Relationships (J. Kornprobst, ed.). *Proc. 3rd Int. Kimberlite Conf.*, 257-264. Elsevier, New York.

CARSWELL, D.A. (1975): Primary and secondary phlogopites and clinopyroxenes in garnet lherzolites. *Phys. Chem. Earth* **9**, 417-429.

______ (1980): Mantle-derived lherzolite nodules associated with kimberlite, carbonatite and basalt magmatism: a review. *Lithos* **13**, 121-138.

______ & GIBB, F.G.F. (1980): Geothermometry of garnet lherzolite nodules with special reference to those from the kimberlites of northern Lesotho. *Contr. Mineral. Petrology* **74**, 403-416.

DAWSON, J.B. (1981): The nature of the upper mantle. *Mineral. Mag.* **44**, 1-18.

______, GURNEY, J.J. & LAWLESS, P.J. (1975): Paleogeothermal gradients derived from xenoliths in kimberlite. *Nature* **257**, 299-300.

______ & STEPHENS, W.E. (1975): Statistical classification of garnets from kimberlite and associated xenoliths. *J. Geol.* **83**, 589-607.

DELANEY, J.S., SMITH, J.V., CARSWELL, D.A. & DAWSON, J.B. (1980): Chemistry of micas from kimberlites and xenoliths. II. Primary- and secondary-textured micas from peridotite xenoliths. *Geochim. Cosmochim. Acta* **44**, 857-872.

ELLIS, D.J. & GREEN, D.H. (1979): An experimental study of the effect of Ca upon garnet–clinopyroxene equilibria. *Contr. Mineral. Petrology* **71**, 13-22.

FABRIÈS, J. (1979): Spinel–olivine geothermometry in peridotites from ultramafic complexes. *Contr. Mineral. Petrology* **69**, 329-336.

FINNERTY, A.A. & BOYD, F.R. (1984): Evaluations of thermobarometers for garnet peridotites. *Geochim. Cosmochim. Acta* **48**, 15-27.

______ & ______ (1987): Thermobarometry for garnet peridotite xenoliths: a basis for upper mantle stratigraphy. *In* Mantle Xenoliths (P.H. Nixon, ed.). John Wiley and Sons Inc., New York (in press).

GOETZE, C. (1975): Sheared xenoliths from the point of view of rock mechanics. *Geology* **3**, 172-173.

GREEN, H.W., II & GUEGUEN, Y. (1974): Origin of kimberlite pipes by diapiric upwelling in the upper mantle. *Nature* **249**, 617-620.

GURNEY, J.J. & HARTE, B. (1980): Chemical variations in upper mantle nodules from South African kimberlites. *Phil. Trans. Roy. Soc. London* **297A**, 273-293.

HARTE, B. (1977): Rock nomenclature with particular relation to deformation and recrystallization textures in olivine-bearing xenoliths. *J. Geol.* **85**, 279-288.

______, COX, K.G. & GURNEY, J.J. (1975): Petrography and geological history of upper mantle xenoliths from the Matsoku kimberlite pipe. *Phys. Chem. Earth* **9**, 477-506.

HEARN, B.C. & MCGEE, E.S. (1984): Garnet peridotites from Williams kimberlites, north-central Montana, U.S.A. *In* Kimberlites II: The Mantle and Crust-Mantle Relationships (J. Kornprobst, ed.). *Proc. 3rd Int. Kimberlite Conf.*, 57-70. Elsevier, New York.

IRVINE, T.N. (1965): Chromian spinel as a petrogenetic indicator. I. Theory. *Can. J. Earth Sci.* **2**, 648-672.

JAGO, B.C. (1982): *Mineralogy and Petrology of the Ham Kimberlite, Somerset Island, N.W.T., Canada.* M.Sc. thesis, Lakehead Univ., Thunder Bay, Ont.

______ & MITCHELL R.H. (1985): Mineralogy and petrology of the Ham kimberlite, Somerset Island, Northwest Territories. *Can. Mineral.* **23**, 619-634.

KENNEDY, C.S. & KENNEDY, G.C. (1976): The equilibrium boundary between graphite and diamond. *J. Geophys. Res.* **81**, 2467-2470.

KRETZ, R. (1966): Interpretation of the shape of mineral grains in metamorphic rocks. *J. Petrology* **7**, 68-94.

LAZ'KO, YE. YE. & SERENKO, V.P. (1984): Peridotites with zoned garnets from Yakutian kimberlites: evidence for deep high-temperature metasomatism and mantle diapirism. *Int. Geol. Rev.* **26**, 318-331.

LINDSLEY, D.H. & DIXON, S.A. (1976): Diopside–enstatite equilibria at 850° to 1400°C, 5 to 35 kb. *Amer. J. Sci.* **276**, 1285-1301.

MACGREGOR, I.D. (1975): Petrologic and thermal structure of the upper mantle beneath South Africa in the Cretaceous. *Phys. Chem. Earth* **9**, 455-466.

MITCHELL, R.H. (1976): Kimberlites of Somerset Island, District of Franklin. *Geol. Surv. Can. Pap.* **76-1A**, 501-502.

______ (1978): Garnet lherzolites from Somerset Island, Canada and aspects of the nature of perturbed geotherms. *Contr. Mineral. Petrology* **67**, 341-347.

______ (1984): Garnet lherzolites from the Hanaus–I and Louwrensia kimberlites of Namibia. *Contr. Mineral. Petrology* **86**, 178-188.

______ (1987): Xenoliths in Canada. *In* Mantle Xenoliths (P.H. Nixon, ed.). John Wiley & Sons Inc., New York (in press).

______, CARSWELL, D.A. & CLARKE, D.B. (1980): Geological implications and validity of calculated equilibration conditions for ultramafic xenoliths from the Pipe 200 kimberlite, northern Lesotho. *Contr. Mineral. Petrology* **72**, 205-217.

MORI, T. & GREEN, D.H. (1978): Laboratory duplication of phase equilibria observed in natural garnet lherzolites. *J. Geol.* **86**, 83-97.

NICKEL, K.G. & BREY, G. (1984): Subsolidus orthopyroxene–clinopyroxene systematics in the system CaO–MgO–SiO_2 to 60 kbar: a re-evaluation of the regular solution model. *Contr. Mineral. Petrology* **87**, 35-42.

NIXON, P.H. & BOYD, F.R. (1973): Petrogenesis of the granular and sheared ultrabasic nodule suite in kimberlite. *In* Lesotho Kimberlites (P.H. Nixon, ed.). Lesotho National Development Corp., Maseru, Lesotho.

______ & ______ (1979): The S.E. Lesotho - E. Griqualand kimberlite field and the nature of the edge cratonic lithosphere. *Proc. De Beers Kimberlite Symp.* (Cambridge), *Extended abstr.*

OBATA, M. (1980): The Ronda peridotite: garnet-, spinel-, plagioclase-lherzolite facies and the P-T trajectories of a high temperature mantle intrusion. *J. Petrology* **21**, 533-572.

O'HARA, M.J., RICHARDSON, S.W. & WILSON, G. (1971): Garnet peridotite stability and occurrence in crust and mantle. *Contr. Mineral. Petrology* **32**, 48-68.

O'NEILL, H.St.C. & WOOD, B.J. (1979): An experimental study of Fe-Mg partitioning between garnet and olivine and its calibration as a geothermometer. *Contr. Mineral. Petrology* **70**, 59-70.

ROEDER, P.L., CAMPBELL, I.H. & JAMIESON, H.E. (1979): A re-evaluation of the olivine-spinel geothermometer. *Contr. Mineral. Petrology* **68**, 325-334.

SCHANDL, E.S. & CLARKE, D.B. (1982): Metasomatism in mantle beneath Pipe 200, northern Lesotho. *Terra Cognita* **2**, 265-266.

SMITH, D. & EHRENBERG, S.N. (1984): Zoned minerals in garnet peridotite nodules from the Colorado Plateau: implications for mantle metasomatism and kinetics. *Contr. Mineral. Petrology* **86**, 274-285.

SPENCE, D.A. & TURCOTTE, D.L. (1985): Magma driven propagation of cracks. *J. Geophys. Res.* **90**, 575-580.

SPERA, F.J. (1981): Carbon dioxide in igneous petrogenesis. II. Fluid dynamics of mantle metasomatism. *Contr. Mineral. Petrology* **77**, 56-65.

______ (1984): Carbon dioxide in igneous petrogenesis. III. Role of volatiles in the ascent of alkaline magma with specific reference to xenolith-bearing mafic lavas. *Contr. Mineral. Petrology* **88**, 217-232.

WELLS, P.R.A. (1977): Pyroxene thermometry in simple and complex systems. *Contr. Mineral. Petrology* **62**, 129-139.

WOOD, B.J. (1974): The solubility of alumina in orthopyroxene coexisting with garnet. *Contr. Mineral. Petrology* **46**, 1-15.

Received June 6, 1986, revised manuscript accepted November 8, 1986.